ARTICLE 1

Spindle assembly without spindle pole body insertion into the nuclear envelope in fission yeast meiosis

Chromosoma

2019

Graphical abstract

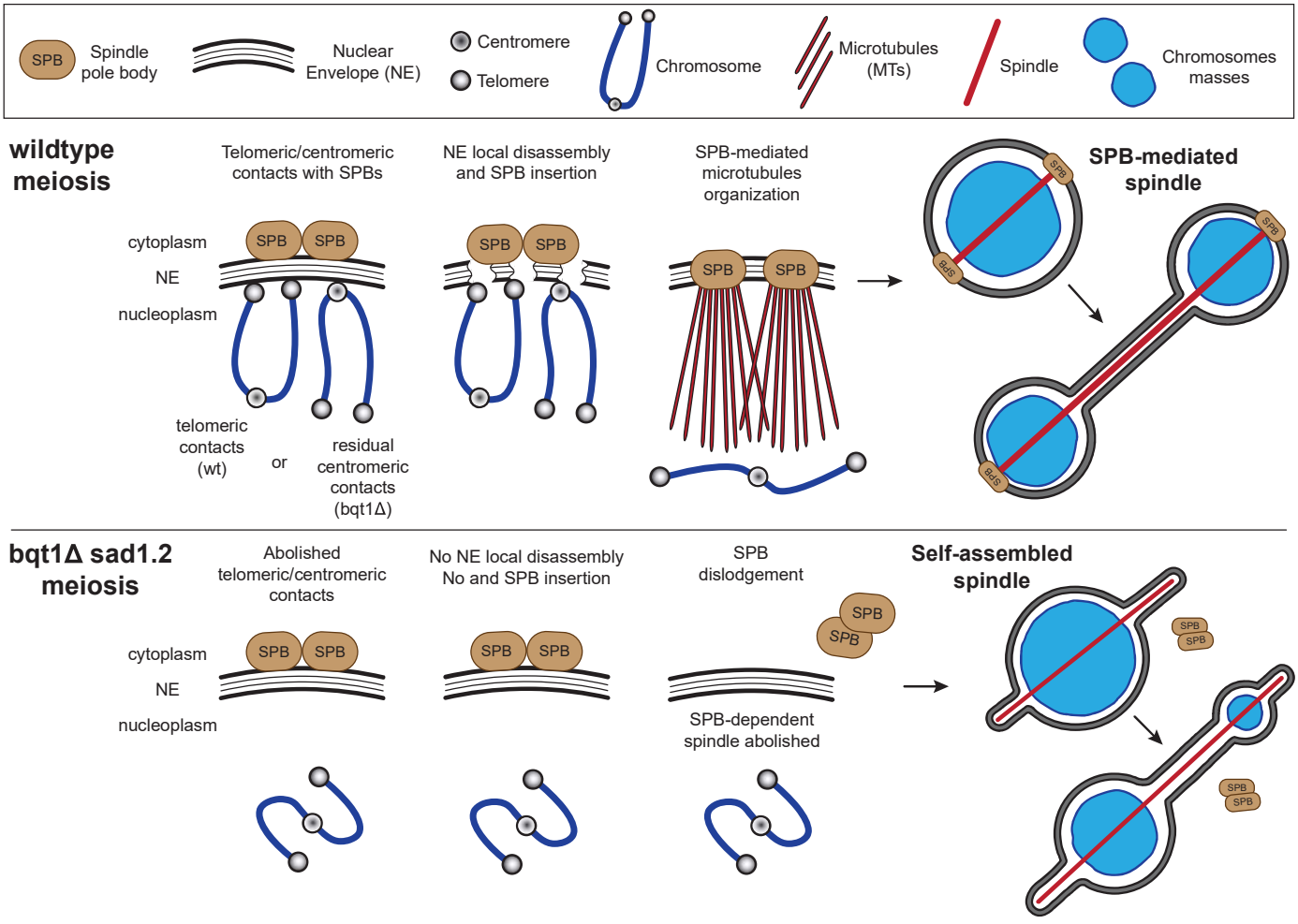

Chromosoma (2019) 128:267–277
https://doi.org/10.1007/s00412-019-00710-y

ORIGINAL ARTICLE

Spindle assembly without spindle pole body insertion into the nuclear envelope in fission yeast meiosis

Alberto Pineda-Santaella [1,2] · Alfonso Fernández-Álvarez [1,2]

Received: 7 November 2018 / Revised: 9 May 2019 / Accepted: 16 May 2019 / Published online: 1 June 2019

Abstract

Centrosomes represent the major microtubule organizing center (MTOC) in eukaryotic cells and are responsible for nucleation of the spindle, the vehicle of chromosome segregation. In human female meiosis, however, spindle assembly occurs in the absence of centrosomes or other MTOCs and microtubules are nucleated around chromosomes. In yeast, spindle formation in mitosis and meiosis depends on the activity of spindle pole bodies (SPBs), the functional equivalents of centrosomes; thus, SPBs and centrosomes use similar machineries to assemble spindles. Here, we develop a system to explore the molecular mechanisms supporting acentrosomal spindle formation using fission yeast meiosis as a model scenario. We achieve this situation by removing access of the SPBs to the nucleus after their duplication. Under these conditions, we observe self-assembly-based spindle formation in the nuclear environment, conferring an ability to segregate chromosomes independently of the SPBs. Our results open the possibility to utilize the experimental advantages of fission yeast for insights into the molecular basis of acentrosomal spindle formation in meiosis.

Keywords Spindle · Meiosis · Fission yeast · Centrosome · Spindle pole body

Introduction

Faithful chromosome segregation depends, in most of metazoa, on the precise action of centrosomes, the major microtubule organizing centers (MTOCs). Centrosomes establish the poles of mitotic spindles and delineate its microtubule axis, which guides the distribution of chromosomes into the daughter cells (Pavin and Tolic 2016). In general, centrosomes contain a pair of centrioles embedded in pericentriolar material, a matrix of proteins required to nucleate and anchor microtubules (Vertii et al. 2016). Defects in activity and regulation of centrosomes lead to alterations in spindle formation, for instance, monopolar or multipolar spindles, and consequently, errors in chromosome segregation and aneuploidy (Nam et al. 2015).

Despite the relevance of centrosomes for cell cycle progression, most metazoan oocytes eliminate their centrosomes during oogenesis (Hertig and Adams 1967; Mikeladze-Dvali et al. 2012; Pimenta-Marques et al. 2016; Szollosi et al. 1972). The centrosome is re-established upon fertilization thanks to sperm components that prompt its construction in the cytoplasm of the zygote (Courtois et al. 2012). Several possible explanations have been proposed for why oocytes lack centrosomes (Manandhar et al. 2005); for instance, it is thought that oocytes remove centrosomes to prevent the coexistence of more than one centrosome after fertilization, which would lead to multipolar spindles and, consequently, chromosome segregation defects (Rodrigues-Martins et al. 2008; Severson et al. 2016); another explanation might be to provide extra constraint on initiation of parthenogenesis, since centrioles are sufficient to trigger the mitotic cycle in unfertilized oocytes (Tournier et al. 1989). For all these reasons, elimination of centrosomes in the female germ line is an important event for ensuring the success of meiosis (Pimenta-Marques et al. 2016).

This article is part of a Special Issue on Recent advances in meiosis from DNA replication to chromosome segregation edited by Valérie Borde and Francesca Cole, co-edited by Paula Cohen and Scott Keeney.

Electronic supplementary material The online version of this article (https://doi.org/10.1007/s00412-019-00710-y) contains supplementary material, which is available to authorized users.

✉ Alfonso Fernández-Álvarez
aferalv@upo.es

[1] Andalusian Center for Developmental Biology (CABD), Pablo de Olavide University/CSIC/Junta de Andalucía, Ctra. Utrera Km.1, 41013 Seville, Spain

[2] Department of Molecular Biology and Biochemical Engineer, Pablo de Olavide University, Ctra. Utrera Km.1, 41013 Seville, Spain

The fact that oocytes of most animal species complete the two rounds of meiotic divisions without centrosomes indicates that meiotic spindles must self-assemble without their canonical reference point (see Fig. 1a). Because of this, microtubule assembly in the absence of centrosomes necessitates a different strategy for nucleation and organization. In this scenario, chromatin plays the active role in spindle formation, establishing the appropriate microenvironment to organize microtubule nucleation (Heald et al. 1996). Spindles formed around chromatin without centrosomes are referred to as acentrosomal spindles.

Molecular mechanisms behind meiotic acentrosomal spindles assembly are much less established than those supporting mitotic spindles. One of the reasons for this lack of knowledge is the limited availability of oocytes for research. Despite these difficulties, it is known from studies in various model systems that the chromatin-bound protein RCC1 (Regulator of Chromosome Condensation) plays an essential role in chromatin-dependent microtubule assembly. RCC1 is the G-nucleotide exchange factor for the Ran system on chromatin; it transforms RanGDP to RanGTP, which activates spindle assembly elements (Carazo-Salas et al. 1999; Clarke and Zhang 2008; Halpin et al. 2011). It has been also described that spindle formation without centrosomes is stabilized by the role of the Ran target, Rae1 (Blower et al. 2005). In addition, cytoskeleton elements like dynein, kinesin (Walczak et al. 1998), and actin are also contributing to chromatin-mediated spindle formation in meiosis (Mogessie and Schuh 2017).

Spindle nucleation in yeast meiosis depends on the spindle pole bodies (SPBs, centrosome-equivalent structure); in contrast to female meiosis in animals, SPBs support spindle formation in meiosis as well as mitosis (Fig. 1a). In fission yeast, SPBs are sitting on the nuclear envelope (NE) in interphase, and for each cell cycle, the NE must be disassembled beneath the SPBs in order to allow the access of microtubules to the chromosomes (Ding et al. 1997; Fernandez-Alvarez and Cooper 2017) (Fig. 1b); this well-controlled process is known as SPB insertion into the NE, and it is the nuclear envelope breakdown (NEBD)-equivalent event in fission yeast (Fernandez-Alvarez et al. 2016; Makarova and Oliferenko 2016). With the aim of disclosing the molecular mechanisms that substantiate acentrosomal spindle formation in meiosis, we have optimized a system to study the behavior of chromatin-dependent spindle formation in meiosis using the fission yeast *Schizosaccharomyces pombe*. This system is based on a combination of mutations which abolishes NE disassembly and, consequently, SPB insertion in almost 100% of cells (Fernandez-Alvarez et al. 2016). Remarkably, in this scenario of the absence of SPB insertion, microtubules show the ability to organize into spindles with the capacity to segregate chromosomes, which resembles the acentrosomal spindle formation in higher eukaryotes. Hence, this study demonstrates that microtubules can be organized around chromosomes in fission yeast in the absence of "active" SPBs and it opens up the possibility to explore, using the genetic and technical advantages of a yeast model, the molecular mechanisms controlling meiotic spindle formation in the absence of centrosomes.

Fig. 1 *bqt1Δ sad1.2* meiotic cells do not show proper spindle formation in a wide range of temperatures. **a** Comparison of microtubule organization in mammals mitosis and female meiosis, i.e., centrosomal and acentrosomal spindles, respectively. During mitosis in higher eukaryotes, centrosomes, the major microtubule organizing center in eukaryotic cells nucleates the spindle to segregate the chromosomes. In order to reach the chromosomes, the nuclear envelope (NE) must be disassembled during a regulated process called nuclear envelope breakdown (NEBD). In contrast, centrosomes are eliminated in female meiosis oocytes and spindles are organized around the chromosomes. In yeast mitosis and mitosis, the spindle pole bodies (SPBs) are responsible of microtubule nucleation and spindle formation during cell division. SPB access to nuclear environment by an analogous process to NEBD denominated SPB insertion into the NE. **b** In fission yeast, SPB insertion into the NE necessitates localized NE disassembly beneath the SPB which is regulated by previous chromosome-NE contacts (Fernandez-Alvarez et al. 2016). Loss of the chromosome-NE contacts by using *sad1.2* allele together with the loss of the meiotic-specific protein Bqt1 fully abolishes NE disassembly and, consequently, the SPB insertion process in around 100% of cells. **c**–**e** Frames from films of meiosis for meiotic chromosomal organization in *wt* and bouquet-deficient cells. Hht1-CFP (histone H3 tagged at one of the two endogenous *hht1*$^{+}$ loci; chromosomes), Sid4-mCherry (endogenously tagged; SPB), ectopically expressed mCherry-atb2 (Tubulin), and Mis6-GFP marking the centromere. Numbers underneath indicate time (minutes) from meiosis I onset. Scale bars represent 5 μm. Schematic for each chromosomal organization is shown on the left. **c** In *wt* cells, prophase stage, characterized by horsetail movement thanks to telomeres cluster beneath the SPB to form the bouquet, is followed by spindle formation in MI and MII which leads to equal chromosome segregation into four haploid cells (spores). Centromeres do not interact with the SPB during meiotic prophase in a *wt* setting. **d** In bouquet mutant cells (*bouquetΔ*), telomeres detach from the SPB. *bouquetΔ* cells (*bqt1* deletion) show no telomere bouquet formation during prophase, chromosomes cannot follow the SPB movement, and the SPB is able to duplicate but not separate in MI and MII due to a failure in the SPB insertion process. Consequently, proper spindle formation is fully abolished. **e** In around 50% of bouquet-mutant cells, centromeres contact with the SPB during prophase trigger SPB insertion into the NE and spindle formation (Fennell et al. 2015). Hence, alternative centromere-SPB contacts emerge to trigger NE disassembly and spindle formation. Yellow arrowheads indicate clear centromere-SPB contact during prophase. **f** Quantitation of the phenotypes shown in **e** at different temperatures (25–33 °C) in *bqt1Δ sad1.2* meiotic cells. Centromere-SPB interactions are reduced in *bqt1Δ* cells by introducing *sad1.2* allele. Analysis of centromere contacts was performed by time-lapse images of 5-min intervals. *wt* and *bqt1Δ* cells were analyzed at 27 °C as controls. *N* is the total number of cells scored from more than two independent experiments. Data were subject to Fisher's exact test: ****$P < 0.0001$; ***$0.0001 < P < 0.001$. **g** Quantitation of proper spindle formation in *wt* and *bqt1Δ sad1.2* cells at different temperatures (25–33 °C). Total number of cells (*N*) is shown, and statistical analysis was performed as in **f**. **h**, **i** Frames from films of *wt* and *bqt1Δ sad1.2* meiotic cells at 31 °C carrying Hht1-CFP (histone H3 tagged at one of the two endogenous *hht1*$^{+}$ loci; Chromosomes), Sid4-mCherry (endogenously tagged; SPB), and ectopically expressed mCherry-atb2 (Tubulin). Yellow arrowhead indicates a failure in the separation of the SPBs. Numbers underneath show time in minutes from meiosis I onset. Scale bars represent 5 μm

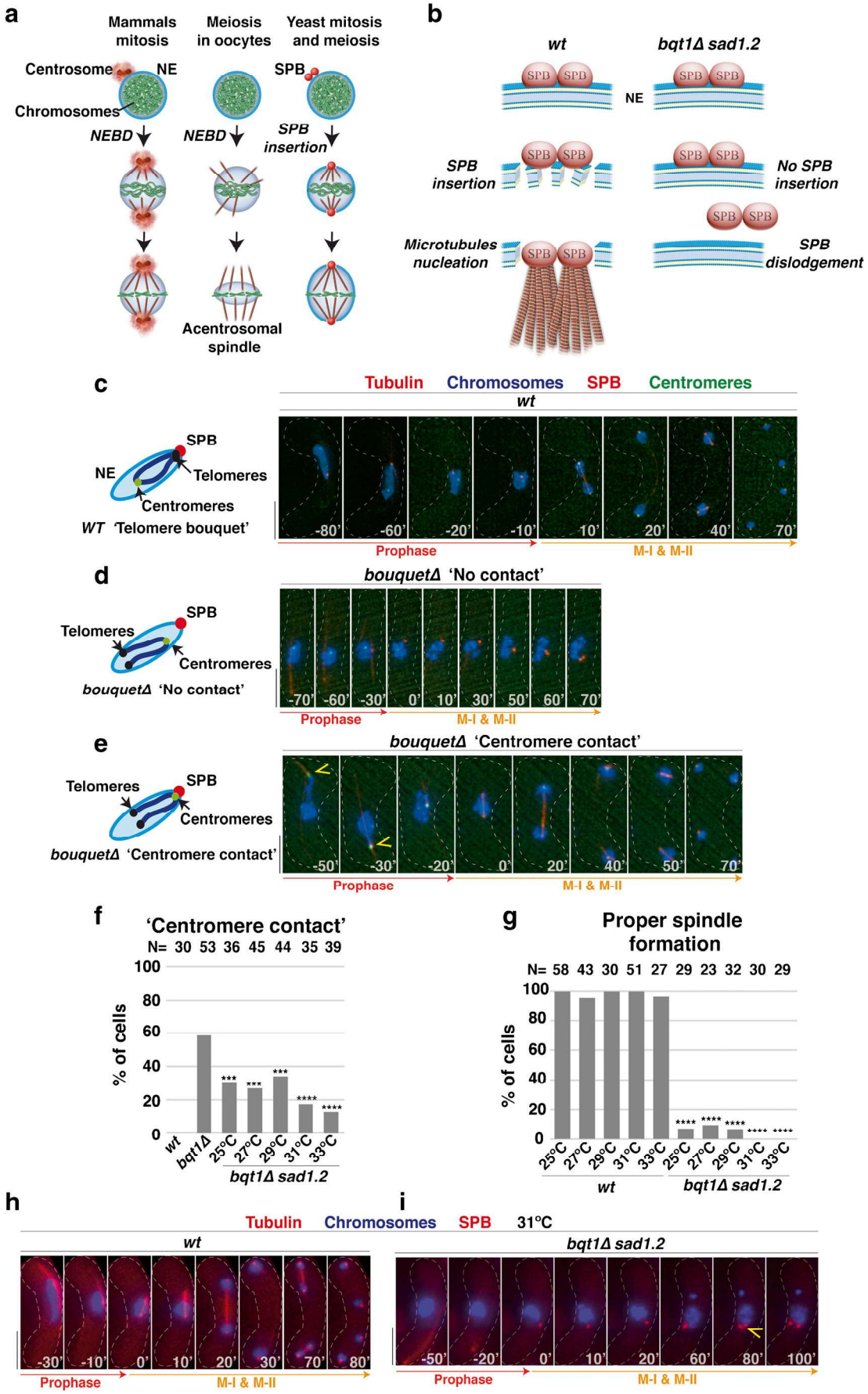
a
Mammals mitosis
Meiosis in oocytes
Yeast mitosis and meiosis
Centrosome
NE
SPB
Chromosomes
NEBD
NEBD
SPB insertion
Acentrosomal spindle
b
wt
bqt1Δ sad1.2
SPB
NE
SPB insertion
No SPB insertion
Microtubules nucleation
SPB dislodgement
c
Tubulin Chromosomes SPB Centromeres
wt
SPB
NE
Telomeres
Centromeres
WT 'Telomere bouquet'
-80' -60' -20' -10' 10' 20' 40' 70'
Prophase
M-I & M-II
d
bouquetΔ 'No contact'
SPB
Telomeres
Centromeres
bouquetΔ 'No contact'
-70' -60' -30' 0' 10' 30' 50' 60' 70'
Prophase
M-I & M-II
e
bouquetΔ 'Centromere contact'
Telomeres
SPB
Centromeres
bouquetΔ 'Centromere contact'
-50' -30' -20' 0' 20' 40' 50' 70'
Prophase
M-I & M-II
f
'Centromere contact'
N= 30 53 36 45 44 35 39
% of cells
wt bqt1Δ 25°C 27°C 29°C 31°C 33°C
bqt1Δ sad1.2
g
Proper spindle formation
N= 58 43 30 51 27 29 23 32 30 29
% of cells
25°C 27°C 29°C 31°C 33°C 25°C 27°C 29°C 31°C 33°C
wt
bqt1Δ sad1.2
h
Tubulin Chromosomes SPB 31°C
wt
-30' -10' 0' 10' 20' 30' 70' 80'
Prophase
M-I & M-II
i
bqt1Δ sad1.2
-50' -20' 0' 10' 20' 60' 80' 100'
Prophase
M-I & M-II

Results and discussion

Optimization of meiotic parameters to study acentrosomal spindle formation in fission yeast

To address the question of whether chromosomes are able to organize spindles in fission yeast meiosis independently of the SPBs, we examined the properties of mutants showing impaired SPB insertion to determine whether there is a microtubule organization activity that might emanate from chromosomes in a manner reminiscent of metazoan oocytes. SPB insertion can be disturbed by the loss of SPB components like Cut12, Cut11, or Brr6, which coordinate cell cycle progression with insertion of SPBs into the NE. However, while mutants in all these proteins show defects in SPB activation and insertion, NE disassembly beneath the SPBs seems to be normally triggered, and frequently one of the SPBs is embedded in the NE, leading to monopolar spindle formation (Tallada et al. 2009; Tamm et al. 2011; West et al. 1998). In order to generate a scenario where SPBs and chromosomes are permanently disconnected by the NE throughout cell cycle, we studied the behavior of mutants where the NE disassembly process is fully abolished. In this context, it has been recently observed in *S. pombe* that NE disassembly in mitosis and meiosis requires previous chromatin-NE contacts during interphase. In particular, loss of the telomere bouquet, the meiotic-specific chromosomal configuration where telomeres cluster together at the NE beneath the centrosome during meiotic prophase, compromises NE disassembly and SPB insertion during meiosis (Fennell et al. 2015; Fernandez-Alvarez et al. 2016). Telomere bouquet formation is achieved by expression of the meiotic-specific proteins Bqt1 and Bqt2, which form a bridge between telomeric proteins and the SUN-domain protein Sad1, located at the inner nuclear membrane (Chikashige et al. 2006). Deletion of *bqt1* or *bqt2* abolishes the telomere bouquet formation and, consequently, the premeiotic telomere-NE contacts required for NE disassembly (Fernandez-Alvarez et al. 2016; Tomita and Cooper 2007). Nevertheless, centromeres can be substitutes for telomeres in the absence of the bouquet, and, for this reason, centromere-NE contacts can also trigger NE disassembly in *bqt1Δ* cells (Fig. 1c–e) (Fennell et al. 2015). To avoid "centromere contacts" in bouquet-deficient cells and generate complete loss of chromatin-NE interactions and consequently, abolish SPB insertion, we combined deletion of *bqt1* together with a thermo-sensitive version of Sad1, Sad1.2 (*bqt1Δ sad1.2* cells). Sad1 connects centromeres and telomeres with the NE (Hagan and Yanagida 1995) and Sad1.2 harbors two substitutions on its N-terminal region, Thr-3-Ser, and Ser-52-Pro, which together disrupt the connection between Sad1 and centromeres when *sad1.2* cells are grown at restrictive temperatures (Fernandez-Alvarez et al. 2016). In order to optimize growth conditions that reduce the number of centromere-NE interactions in *bqt1Δ sad1.2* cells, we first analyzed the state of centromere-NE interactions in *bqt1Δ sad1.2* cells at different temperatures: 25 °C, 27 °C, 29 °C, 31 °C, and 33 °C (see "Methods"); higher temperatures showed problems in the triggering and progression of meiosis. As can be observed in Fig. 1f, the percentage of *bqt1Δ* cells showing centromere-NE contacts significantly decreases by introducing *sad1.2* allele into a *bqtΔ* setting even at 25 °C. Consistently with previous data in mitosis where more penetrant effects of Sad1.2 on centromere clustering occur at higher temperatures (Fernandez-Alvarez et al. 2016), this decrease is more obvious at 31 °C and 33 °C, suggesting that around these temperatures, Sad1.2 suffers a conformational change which leads to disruption of its interaction with centromeres.

Loss of telomere/centromere-NE interaction leads to defective NE disassembly and consequently, defective spindle formation. Congruently, quantification of proper spindle formation in *bqt1Δ sad1.2* meiosis showed such defects at all temperatures tested; notably, we found 100% penetrance of defects at 31 °C and 33 °C, consistent with the reduction of centromere-SPB interactions at these temperatures. Interestingly, we found that although centromere contacts at 25 °C, 27 °C, and 29 °C occur in around 30% of cells, proper spindle formation is only found in less than 10% of the population (Fig. 1g). There is a tight correlation between the longevity of prophase chromatin-Sad1 contacts and proper spindle formation; in this context, Sad1.2 mutations are additionally affecting longevity of centromere-NE interactions. Thus, *bqt1Δ sad1.2* cells show not only a reduced but also a less stable number of centromere contacts throughout meiosis. An example of *bqt1Δ sad1.2* meiotic progression at 31 °C is shown in Fig. 1i. In *wt* cells, horsetail movement during prophase is followed by proper spindle formation in meiosis I (MI) and meiosis II (MII), which leads to the generation of four equal masses of chromatin (Fig. 1h). In contrast, due to loss of the telomere bouquet (*bqt1Δ*), the fluctuating SPB during prophase lacks contact with telomeres and the *sad1.2* allele prevents centromere-NE interactions; for this reason, the horsetail movement is abolished in *bqt1Δ sad1.2* cells and, although SPBs are able to duplicate, their separation is compromised due to an unsuccessful SPB insertion into the NE as previously demonstrated (Fernandez-Alvarez et al. 2016) (yellow arrow in Fig. 1i). In this scenario, proper spindle formation is abolished in around 100% of *bqt1Δ sad1.2* cells.

Fig. 2 Spindle self-assembly in the absence of "active" SPBs in fission yeast meiosis. **a**–**f** Frames from films of *wt* and *bqt1Δ sad1.2* meiosis at 31 °C harboring the specified tags: tubulin and chromosomes tagged as in Fig. 1. Cut12-GFP, Sid4-GFP, and Pcp1-GFP, endogenously tagged, were used as SPB markers. Scale bars represent 5 μm. Self-assembled spindle formation independent of the SPBs can be observed in *bqt1Δ sad1.2* cells (**b**, **d**, **f**). **g** Quantitation of self-assembled spindles in the absence of SPB insertion. *N* is the total number of cells scored from more than two independent experiments at 31 °C. Data were subject to Fisher's exact test: ****$P < 0.0001$

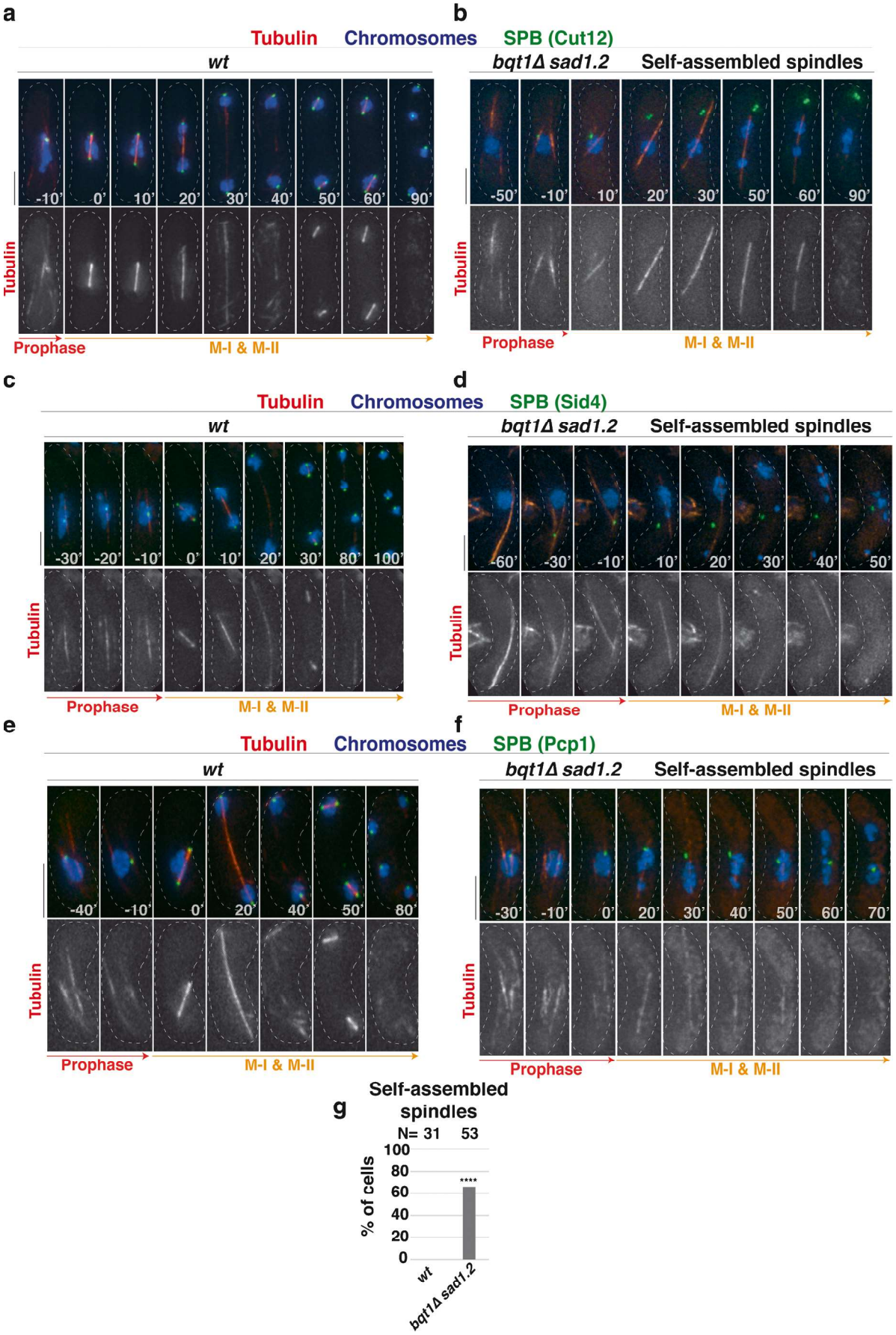
a
Tubulin Chromosomes SPB (Cut12)
wt
-10' 0' 10' 20' 30' 40' 50' 60' 90'
Tubulin
Prophase
M-I & M-II
b
bqt1Δ sad1.2 Self-assembled spindles
-50' -10' 10' 20' 30' 50' 60' 90'
Tubulin
Prophase
M-I & M-II
c
Tubulin Chromosomes SPB (Sid4)
wt
-30' -20' -10' 0' 10' 20' 30' 80' 100'
Tubulin
Prophase
M-I & M-II
d
bqt1Δ sad1.2 Self-assembled spindles
-60' -30' -10' 10' 20' 30' 40' 50'
Tubulin
Prophase
M-I & M-II
e
Tubulin Chromosomes SPB (Pcp1)
wt
-40' -10' 0' 20' 40' 50' 80'
Tubulin
Prophase
M-I & M-II
f
bqt1Δ sad1.2 Self-assembled spindles
-30' -10' 0' 20' 30' 40' 50' 60' 70'
Tubulin
Prophase
M-I & M-II
g
Self-assembled spindles
N= 31 53
% of cells
100
80
60
40
20
0
****
wt
bqt1Δ sad1.2

Hence, and considering 27 °C as optimal temperature for meiotic studies in fission yeast, we established *bqt1Δ sad1.2* meiosis at 31 °C as the best condition to examine possible spindle formation in the absence of SPB insertion.

Microtubules organize into spindles around chromosomes in the absence of SPB insertion

To pinpoint if the nuclear environment can confer spindle assembly when SPB insertion is compromised, we studied meiotic progression in *bqt1Δ sad1.2* cells at 31 °C. During this analysis, we found that a population of *bqt1Δ sad1.2* cells seemed to be able to separate chromosomes even in the absence of separation of the SPBs, and this phenotype was mediated by microtubules. As we can see in Fig. 2, microtubules are able to organize into spindles in the mutant, with the putative ability to segregate chromosomes (20′ and 30′ in Fig. 2b; 10′ and 20′ in Fig. 2d; and 20′ and 30′ in Fig. 2f). Remarkably, the spindle axis is established independently of SPB localization, suggesting that the mechanism governing acentrosomal spindle formation in higher eukaryotes might be responsible of these phenotypes. These observations were consistent using different SPB markers located at different SPB layers (Bestul et al. 2017) (Fig. 2). Stimulatingly in terms of future studies to decipher the basis for this spindle formation, we found that the rate of spindles self-assembled in the absence of SPB insertion is around 60% (Fig. 2g).

To confirm that spindle self-assembly in *bqt1Δ sad1.2* cells is accomplished inside the nucleus and is not a cytoplasmic event, we followed the behavior of the NE in *bqt1Δ sad1.2* meiosis via the endogenously GFP-tagged Ish1 protein. As shown in Fig. 3b, c, we found that the spindle is clearly formed around chromosomes within the nucleus. Interestingly, the NE is pushed from the inside as a consequence of spindle extension, even when the SPBs are clearly dislodged from the NE (Fig. 3b–d).

These observations strongly suggest that some component within the nucleus is able to trigger spindle assembly in the absence of SPB insertion, resembling the scenario found in female meiosis in most animals. Several studies have demonstrated that kinetochores have the ability to generate microtubules (Kitamura et al. 2010; McGill and Brinkley 1975). We speculate that self-assembly of spindles without SPBs might be supported by key elements already imported inside the nucleus, which might be recruited to the kinetochores, in a cell cycle-regulated manner. These elements might also be necessary for SPB-mediated spindle nucleation; their ability to form spindles in the absence of SPB insertion is unmasked by blocking the partial NEBD required for SPB insertion. In this context, it is known that importin α mediates the trafficking of elements regulating spindle assembly in fission yeast meiosis (Flor-Parra et al. 2018); it would be interesting to determine whether loss of Imp1 alters the formation of acentrosomal spindles in *bqt1Δ sad1.2* cells. Current studies aim to study the role of nuclear import in these phenotypes.

Self-assembled spindles share features with proper spindles but segregate chromosomes with high rate of errors

To illuminate the properties of self-assembled spindles in the absence of SPB insertion, we compared the spindle dynamics in a *wt* setting, in which SPBs nucleate proper spindles, with self-assembled spindles in *bqt1Δ sad1.2* cells. In the absence of SPB insertion, we noticed that self-assembled spindles are able to assemble, extend, and disassemble; in particular, initiation of self-assembled spindles takes around 5–10 min longer compared to those mediated by the SPBs (Fig. 4a). Once spindle formation is triggered, self-assembled spindles reach maximal length of 8.36 ± 0.67 μm ($N = 15$ cells), in contrast to 14.30 ± 0.46 μm ($N = 14$ cells) in *wt* cells (Fig. 4b) (Flor-Parra et al. 2018). Accordingly, we noticed that intensity of alpha tubulin signal is weaker for acentrosomal spindles compared to spindles mediated by the SPBs. Reasons for these differences include two possible scenarios: (i) Gamma tubulin, tubulin, and other nucleation factors might be scarce in the nucleus since SPB insertion or rather, partial NEBD, which is lost in the *bqt1Δ sad1.2* background, might be necessary to import all necessary factors for proper spindle formation; (ii) alternatively, all key elements for the formation of a robust spindle have efficiently been imported inside the nucleus, but without the SPBs inserted into the NE, the reference point to orchestrate the formation of the spindle is lost and then, the process is compromised. In this context, it would be interesting to force the accumulation of tubulin and gamma tubulin complex inside the nucleus in the absence of SPB insertion in *bqt1Δ sad1.2* cells in order to see if the robustness of the spindle can be improved. In line with this idea, it has been shown that forced import of the microtubule-associated protein Alp14/TOG is enough to trigger spindle formation during interphase (Kume et al. 2018).

Despite the weakness of self-assembled spindles, a crucial stabilizing factor of proper spindles, Ase1/PRC1, is also locating in the mid-zone (Fig. 4c), suggesting that at least part of the molecular machinery controlling the SPB-mediated spindle formation might be also somewhat involved in the formation of self-assembled spindles in fission yeast.

To determine if the self-assembled spindles observed in *bqt1Δ sad1.2* cells have the genuine ability to segregate chromosomes, we analyzed the behavior of centromeres during the extension of the spindle in the absence of SPB insertion. As we can observe in Fig. 5a, centromeres (visualized via GFP-tagged Mis6) are captured by the spindle (10′ frame in Fig. 5a) and separated to opposite poles of the cell (30′ frame in Fig. 5a), indicating that the spindle can attach chromosomes. Congruently, sporulation efficiency showed that around 60%

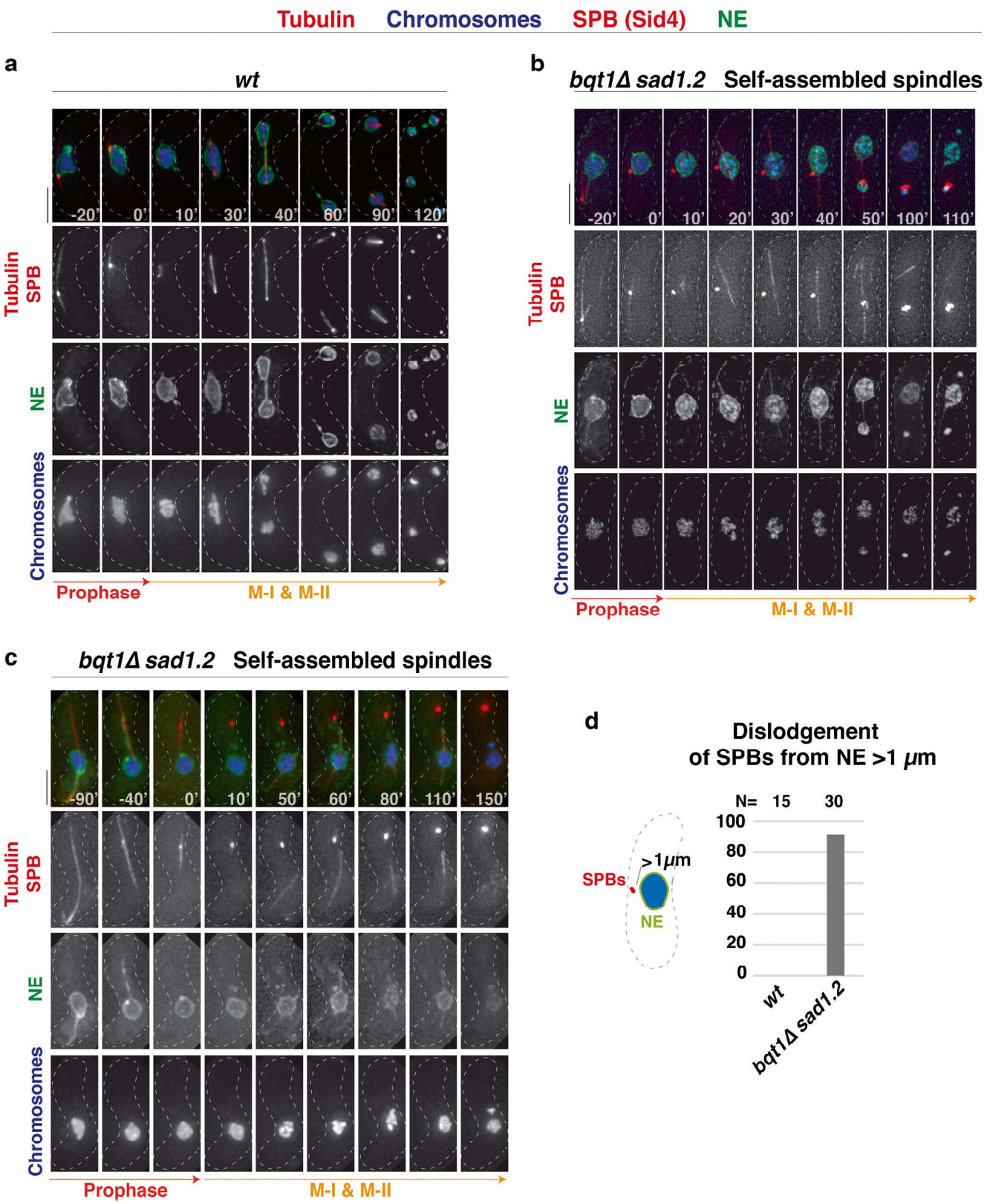

Fig. 3 Spindle self-assembly occurs in the nuclear environment. **a**–**c** Frames of films of *wt* and *bqt1Δ sad1.2* meiosis at 31 °C. SPB is seen via Sid4-mCherry, spindles via ectopically expressed mCherry-Atb2 (*nda3* promoter controlled) and chromosomes (histone H3 tagged at one of the two endogenous *hht1*$^{+}$ loci). Ish1-GFP was used to visualize the NE. Numbers underneath represent time (minutes) from MI onset. Scale bars represent 5 μm. **d** Quantitation of SPB insertion defects shown in **b**, **c**. We defined SPB insertion defect when SPBs locate > 1 μm from the NE as it has been previously described (Fernandez-Alvarez et al. 2016). Dislodgement of the SPB from the NE is never observed in *wt* settings

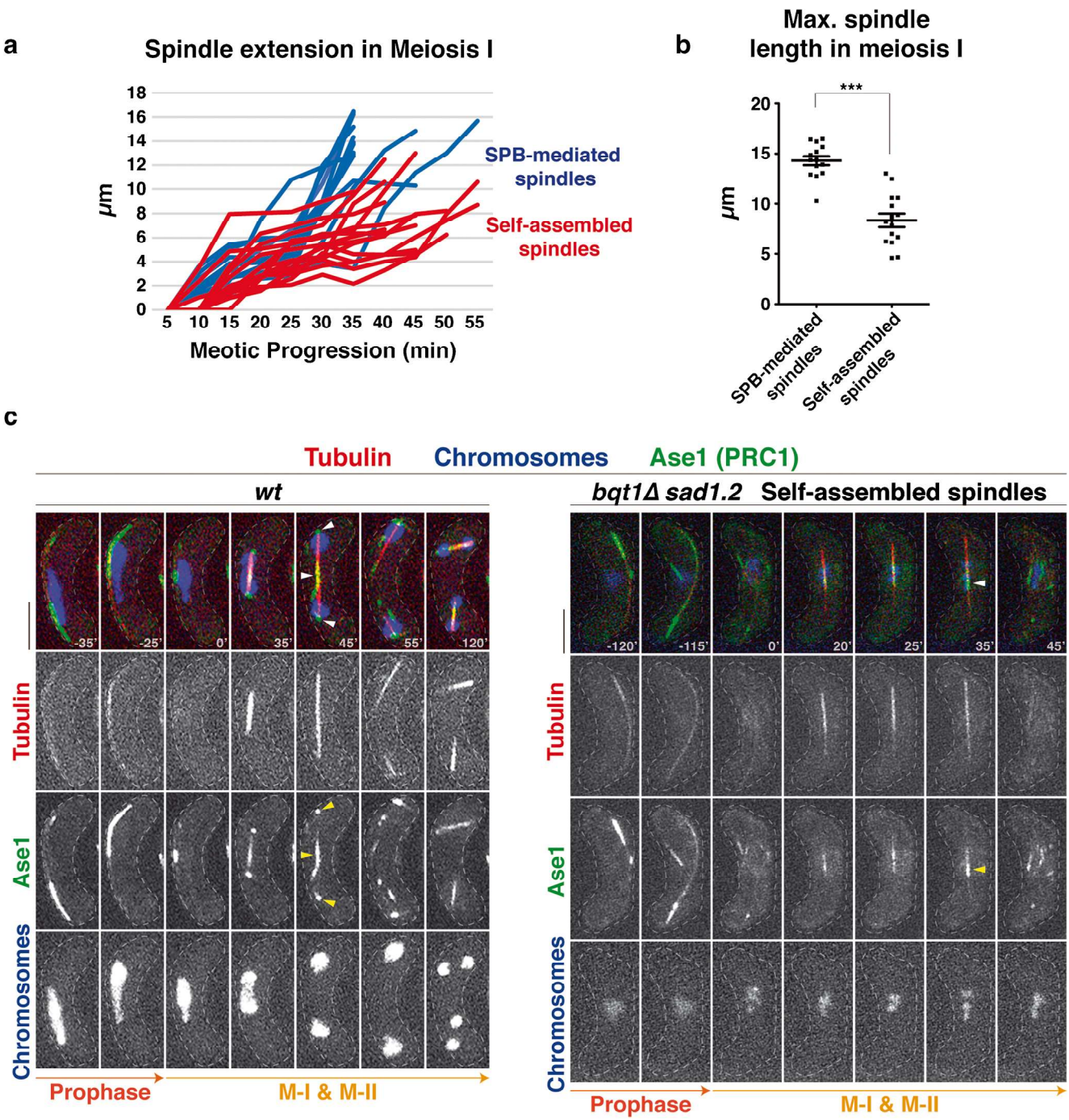

Fig. 4 Self-assembled spindles show similarities with proper spindles. **a** Quantitation of spindle extension in *wt* (SPB-mediated spindles) and *bqt1Δ sad1.2* (self-assembled spindles) cells at 31 °C. Time on *x*-axis starts from the moment when SPB duplication was detected. Each line represents one single cell. **b** Quantitation of maximum spindle length derived from data shown in **a**; mean and SEM are shown. Data were subject to Fisher's exact test: ***$0.0001 < P < 0.001$. **c** Ase1/PRC1 protein localizes to meiotic self-assembled spindles. Frames from films of meiosis. Chromatin and tubulin are viewed as in Fig. 1, Ase1-GFP (endogenously tagged). In *wt* cells, Ase1 protein localizes to the spindle poles and midzone (arrowheads in 45′ frame). In 93% of self-assembled spindles in *bqt1Δ sad1.2* cells, Ase1-GFP also locates to the midzone of the spindle (35′ frame, arrowheads). Scale bar represents 5 µm

of *bqt1Δ sad1.2* asci contained 2, 3, or 4 spores (Fig. 5b, c), which implies events of chromosome distribution. However, we found only around 30% of asci with four equally sized spores (Fig. 5b, c). In line with this observation, we also noticed a high rate of lagging and unsegregated chromosomes (Fig. 5d); approximately 80% of segregations showed such errors (Fig. 5e). Chromosome segregation in human female meiosis has an intrinsically high rate of errors, and one of the

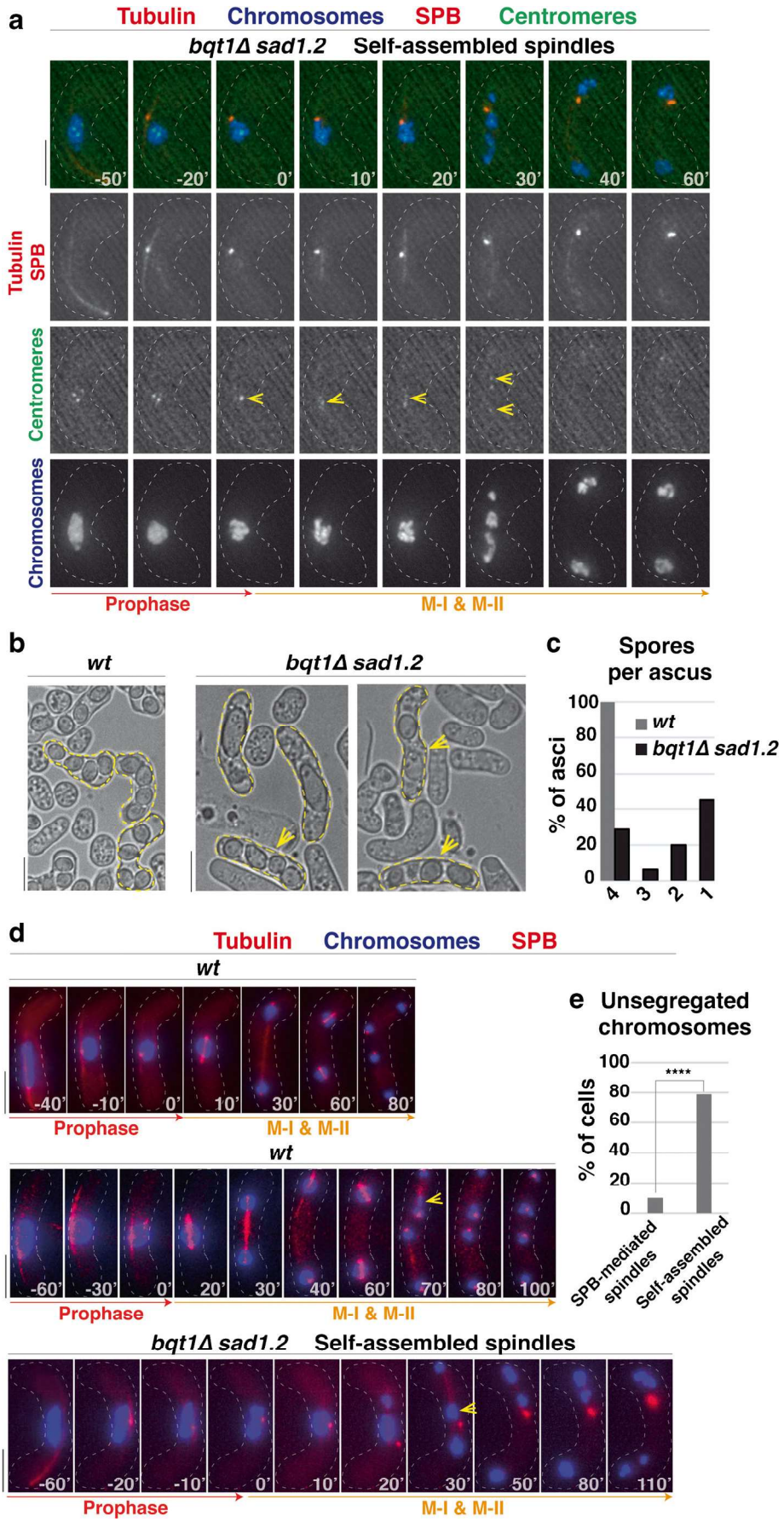

Fig. 5 Self-assembled spindles in the absence of SPB insertion show high rate of failure of chromosome attachment. **a** Frames from films of *bqt1Δ sad1.2* carrying chromatin, SPB and tubulin, viewed as in Fig. 1, and centromeres via endogenously GFP-tagged Mis6. Bar 5 μm. Behavior of centromeres is indicated by yellow arrowheads. **b**, **c** Asci generated from *wt* and *bqt1Δ sad1.2* were analyzed by light microscopy. Data were scored from more than three independent experiments at 31 °C. Yellow arrows point *bqt1Δ sad1.2* asci containing more than one spore suggesting segregation of chromosomes. **d** Series of frames from films of *wt* and *bqt1Δ sad1.2* cells undergoing meiosis. Tags and numbers as in Fig. 1. Scale bars represent 5 μm. Failed spindle attachment for chromosomes is indicated by arrows. **e** Quantitation of the frequency of non-attached chromosome events as observed via tagged histone H3. Data were subject to Fisher's exact test: ****$P < 0.0001$. N is the total number of cells scored from more than two independent experiments

most pertinent reasons is the absence of centrosomes or other MTOCs (Hassold and Hunt 2001; Holubcova et al. 2015; Mogessie et al. 2018). Congruently, the spindle which we observed in *bqt1Δ sad1.2* cells is also very inefficient at segregating chromosomes accurately. With the aim to improve faithful chromosome segregation in acentrosomal meiosis, we are currently trying to identify elements which can improve the robustness of the self-assembled spindles.

Conclusion

In this study, we have observed the formation of self-assembled spindles in the absence of SPB insertion. This phenotype is consistent with the notion that chromatin has the capability to organize microtubules in the absence of centrosomes and other MTOCs.

The conserved ability of components of the nuclear environment to nucleate spindles without centrosomes has been long recognized, and the optimization of a robust and genetically manageable scenario, using fission yeast as model system, is a new powerful tool for deciphering the basis for acentrosomal meiotic spindles.

Methods

Strains, plasmids, and growth conditions

Strains used in this work are listed in Supplementary Table 1. Standard fission yeast and molecular biology approaches (Moreno et al. 1991) were used. Gene deletion and C-terminal tagging were performed as described (Fennell et al. 2015). pFA6a plasmids were used to amplify kanMX6, hphMX6, and natMX6 resistance cassettes. Insertions of mCherry-Atb2 at the *aur1* locus (Hashida-Okado et al. 1998) utilized pYC19-mCherry-Atb2 (Nakamura et al. 2011) provided by T. Toda (Hiroshima University). Final concentrations of aureobasidin A (0.5 μg/mL), nourseothricin (100 μg/mL clonNAT), G418 (150 μg/mL geneticin), and hygromycin B (300 μg/mL) were added for selection purpose.

Meiosis induction and microscopy sample preparation

Homothallic (h^{90}) haploid strains were grown on YES rich medium plates at 32 °C and then were plated on SPA (nitrogen source free media) plates at 28 °C. Live analysis was carried out 6–6.5 h after meiosis induction. Asci formation studies were performed 2 days after meiosis induction.

To prepare the samples for live microscopy, cells were resuspended in 200 μL of milli-Q water and 100 μL of the mixture incubated for 4 min on lectin-coated glass bottom 35-mm dish (Ibidi Gmbh, Germany) at room temperature. To maintain sporulating conditions and ensure meiosis progression, minimal medium without nitrogen was added to the chamber up to a final volume of 3 mL.

Live imaging of meiotic cells and image analysis

Meiotic cells were filmed through fluorescence confocal spinning disk microscopy (Photometrics Evolve camera; Olympus 100 × 1.4 NA oil immersion objective; Roper Scientific) and DeltaVision microscope system (Applied Precision, Seattle, WA). In the case of spinning disk, a timelapse of 61 timepoints of 5 min duration each (5 h) with 13 focal planes of 0.5 μm stepsize each, using 100 ms and 50 ms of exposure for fluorescence and DIC channels, respectively, was conveyed. For analysis using Delta Vision, images were acquired over 26 focal planes at a 0.35 μm step size. For time-lapse imaging at 25 °C, 27 °C, 29 °C, 31 °C, and 33 °C, we used an Environmental Chamber with a DeltaVision Spectris (Applied Precision) comprising an Olympus IX70 widefield inverted epifluorescence microscope, an Olympus UPlanSapo × 100 NA 1.4 oil immersion objective, and a Photometrics CCD CoolSnap HQ camera.

Deltavision images were deconvolved and combined into a 2D image using the maximum intensity projection setting using SoftWorx (Applied Precision). Image processing and analysis were performed using ImageJ and Adobe Photoshop CS5.1.

Acknowledgments We thank Julie Cooper, María Almuedo-Castillo, and Isabel Almudí for critical comments on the manuscript; Yesica García for technical support; and the CABD microscopy facility technician Katherina García for their helpful advice. We would like to thank the Genetics Department for their useful discussions and comments, especially Rafael R. Daga, Juan Jiménez, and Jose Ignacio Ibeas; and Víctor Manuel Carranco Fabre for the graphic design in the figures and technical support.

Funding information This work was supported by Spanish Government (Ramon y Cajal program, RyC-2016-19659) to AF-A; AP-S by Pablo de Olavide University Fellowship (PPI1807). The CABD is an institution funded by Pablo de Olavide University, Consejo Superior de Investigaciones Científicas (CSIC) and Junta de Andalucía.

Abbreviations MI, meiosis I; MII, meiosis II; NE, nuclear envelope; SPB, spindle pole body; NEBD, nuclear envelope breakdown

References

Bestul AJ, Yu Z, Unruh JR, Jaspersen SL (2017) Molecular model of fission yeast centrosome assembly determined by superresolution imaging. J Cell Biol 216:2409–2424

Blower MD, Nachury M, Heald R, Weis K (2005) A Rae1-containing ribonucleoprotein complex is required for mitotic spindle assembly. Cell 121:223–234

Carazo-Salas RE, Guarguaglini G, Gruss OJ, Segref A, Karsenti E, Mattaj IW (1999) Generation of GTP-bound ran by RCC1 is required for chromatin-induced mitotic spindle formation. Nature 400:178–181
Chikashige Y, Tsutsumi C, Yamane M, Okamasa K, Haraguchi T, Hiraoka Y (2006) Meiotic proteins bqt1 and bqt2 tether telomeres to form the bouquet arrangement of chromosomes. Cell 125:59–69
Clarke PR, Zhang C (2008) Spatial and temporal coordination of mitosis by ran GTPase. Nat Rev Mol Cell Biol 9:464–477
Courtois A, Schuh M, Ellenberg J, Hiiragi T (2012) The transition from meiotic to mitotic spindle assembly is gradual during early mammalian development. J Cell Biol 198:357–370
Ding R, West RR, Morphew DM, Oakley BR, McIntosh JR (1997) The spindle pole body of Schizosaccharomyces pombe enters and leaves the nuclear envelope as the cell cycle proceeds. Mol Biol Cell 8: 1461–1479
Fennell A, Fernandez-Alvarez A, Tomita K, Cooper JP (2015) Telomeres and centromeres have interchangeable roles in promoting meiotic spindle formation. J Cell Biol 208:415–428
Fernandez-Alvarez A, Bez C, O'Toole ET, Morphew M, Cooper JP (2016) Mitotic nuclear envelope breakdown and spindle nucleation are controlled by interphase contacts between centromeres and the nuclear envelope. Dev Cell 39:544–559
Fernandez-Alvarez A, Cooper JP (2017) Chromosomes orchestrate their own liberation: nuclear envelope disassembly. Trends Cell Biol 27: 255–265
Flor-Parra I, Iglesias-Romero AB, Salas-Pino S, Lucena R, Jimenez J, Daga RR (2018) Importin alpha and vNEBD control meiotic spindle disassembly in fission yeast. Cell Rep 23:933–941
Hagan I, Yanagida M (1995) The product of the spindle formation gene sad1+ associates with the fission yeast spindle pole body and is essential for viability. J Cell Biol 129:1033–1047
Halpin D, Kalab P, Wang J, Weis K, Heald R (2011) Mitotic spindle assembly around RCC1-coated beads in Xenopus egg extracts. PLoS Biol 9:e1001225
Hashida-Okado T, Yasumoto R, Endo M, Takesako K, Kato I (1998) Isolation and characterization of the aureobasidin A-resistant gene, aur1R, on Schizosaccharomyces pombe: roles of Aur1p+ in cell morphogenesis. Curr Genet 33:38–45
Hassold T, Hunt P (2001) To err (meiotically) is human: the genesis of human aneuploidy. Nat Rev Genet 2:280–291
Heald R, Tournebize R, Blank T, Sandaltzopoulos R, Becker P, Hyman A, Karsenti E (1996) Self-organization of microtubules into bipolar spindles around artificial chromosomes in Xenopus egg extracts. Nature 382:420–425
Hertig AT, Adams EC (1967) Studies on the human oocyte and its follicle. I. Ultrastructural and histochemical observations on the primordial follicle stage. J Cell Biol 34:647–675
Holubcova Z, Blayney M, Elder K, Schuh M (2015) Human oocytes. Error-prone chromosome-mediated spindle assembly favors chromosome segregation defects in human oocytes. Science 348:1143–1147
Kitamura E, Tanaka K, Komoto S, Kitamura Y, Antony C, Tanaka TU (2010) Kinetochores generate microtubules with distal plus ends: their roles and limited lifetime in mitosis. Dev Cell 18:248–259
Kume K, Kaneko S, Nishikawa K, Mizunuma M, Hirata D (2018) Role of nucleocytoplasmic transport in interphase microtubule organization in fission yeast. Biochem Biophys Res Commun 503:1160–1167
Makarova M, Oliferenko S (2016) Mixing and matching nuclear envelope remodeling and spindle assembly strategies in the evolution of mitosis. Curr Opin Cell Biol 41:43–50
Manandhar G, Schatten H, Sutovsky P (2005) Centrosome reduction during gametogenesis and its significance. Biol Reprod 72:2–13
McGill M, Brinkley BR (1975) Human chromosomes and centrioles as nucleating sites for the in vitro assembly of microtubules from bovine brain tubulin. J Cell Biol 67:189–199
Mikeladze-Dvali T, von Tobel L, Strnad P, Knott G, Leonhardt H, Schermelleh L, Gonczy P (2012) Analysis of centriole elimination during C. elegans oogenesis. Development 139:1670–1679
Mogessie B, Scheffler K, Schuh M (2018) Assembly and positioning of the oocyte meiotic spindle. Annu Rev Cell Dev Biol 34:381–403
Mogessie B, Schuh M (2017) Actin protects mammalian eggs against chromosome segregation errors. Science 357:eaal1647
Moreno S, Klar A, Nurse P (1991) Molecular genetic analysis of fission yeast Schizosaccharomyces pombe. Methods Enzymol 194:795–823
Nakamura Y, Arai A, Takebe Y, Masuda M (2011) A chemical compound for controlled expression of nmt1-driven gene in the fission yeast Schizosaccharomyces pombe. Anal Biochem 412:159–164
Nam HJ, Naylor RM, van Deursen JM (2015) Centrosome dynamics as a source of chromosomal instability. Trends Cell Biol 25:65–73
Pavin N, Tolic IM (2016) Self-organization and forces in the mitotic spindle. Annu Rev Biophys 45:279–298
Pimenta-Marques A, Bento I, Lopes CA, Duarte P, Jana SC, Bettencourt-Dias M (2016) A mechanism for the elimination of the female gamete centrosome in Drosophila melanogaster. Science 353:aaf4866
Rodrigues-Martins A, Riparbelli M, Callaini G, Glover DM, Bettencourt-Dias M (2008) From centriole biogenesis to cellular function: centrioles are essential for cell division at critical developmental stages. Cell Cycle 7:11–16
Severson AF, von Dassow G, Bowerman B (2016) Oocyte meiotic spindle assembly and function. Curr Top Dev Biol 116:65–98
Szollosi D, Calarco P, Donahue RP (1972) Absence of centrioles in the first and second meiotic spindles of mouse oocytes. J Cell Sci 11: 521–541
Tallada VA, Tanaka K, Yanagida M, Hagan IM (2009) The S. pombe mitotic regulator Cut12 promotes spindle pole body activation and integration into the nuclear envelope. J Cell Biol 185:875–888
Tamm T, Grallert A, Grossman EP, Alvarez-Tabares I, Stevens FE, Hagan IM (2011) Brr6 drives the Schizosaccharomyces pombe spindle pole body nuclear envelope insertion/extrusion cycle. J Cell Biol 195: 467–484
Tomita K, Cooper JP (2007) The telomere bouquet controls the meiotic spindle. Cell 130:113–126
Tournier F, Karsenti E, Bornens M (1989) Parthenogenesis in Xenopus eggs injected with centrosomes from synchronized human lymphoid cells. Dev Biol 136:321–329
Vertii A, Hehnly H, Doxsey S (2016) The centrosome, a multitalented renaissance organelle. Cold Spring Harb Perspect Biol 8
Walczak CE, Vernos I, Mitchison TJ, Karsenti E, Heald R (1998) A model for the proposed roles of different microtubule-based motor proteins in establishing spindle bipolarity. Curr Biol 8:903–913
West RR, Vaisberg EV, Ding R, Nurse P, McIntosh JR (1998) cut11(+): a gene required for cell cycle-dependent spindle pole body anchoring in the nuclear envelope and bipolar spindle formation in Schizosaccharomyces pombe. Mol Biol Cell 9:2839–2855